DESIGN OF EFFICIENT MAGNETIC COILS FOR REPETITIVE STIMULATION

RADU CIUPA , LAURA DARABANT, MIHAELA PLEŞA, OCTAVIAN CREŢ, DAN DORU MICU

Key words: Magnetic stimulation, Energy transfer, Nerve fibers.

The technique of magnetic stimulation of nerve fibres represents a new direction of research in modern medicine. This study starts from a major limitation of the coils used for magnetic stimulation: their inability to specifically stimulate the target tissue, without activating the surrounding areas. The first goal of this study was to determine the optimal configuration of coils for some specific application. Once the coil configuration established, we address other issues that need to be solved: reducing power consumption and coil heating in order to make a step forward in the direction of repetitive magnetic stimulation.

1. INTRODUCTION

The preoccupation for improving the quality of life, for persons with different handicaps, led to extended research in the area of functional stimulation.

The human nervous system can be stimulated by strong magnetic field pulses that induce an electric field in the tissue, leading to excitation of neurons [1]. A disadvantage consists, however, in the fact that the need of focal stimulation can not always be fulfilled. This is why the design of magnetic coils can help achieving this goal.

The present paper starts by emphasizing the theoretical background of magnetic stimulation, referring to the mathematical model for the computation of the electric field induced in the human tissue during magnetic stimulation. Also, we present a method for the computation of the inductance of magnetic coils. Then, we asses the focality of magnetic coils specially designed to improve this feature of the stimulation – Slinky coils. Finally, we analyze where the turns should be placed, inside the coil, to achieve activation of the nervous fibres with minimum energy cost.

Technical University of Cluj-Napoca, 15 Ctin. Daicoviciu, Cluj-Napoca, Romania; E-mail: Radu.Ciupa@et.utcluj.ro

Rev. Roum. Sci. Techn. – Électrotechn. et Énerg., **55**, *3*, p. 251–260, Bucarest, 2010

2. THEORETICAL BACKGROUND

The current required to induce the electric field (high field strength are required in magnetic stimulation) is delivered by a magnetic stimulator (RLC circuit). The current waveform obtained by discharging a capacitor, with an initial voltage U_0, through the coil is [2]:

$$I = U_0 / \omega L \cdot \sin(\omega t) \exp(-\alpha t), \tag{1}$$

where $\alpha = R/(2L)$, $\omega = \sqrt{1/LC - \alpha^2}$, C is the capacitance, and R $(R < R_{cr})$ and L are the resistance and inductance of the coil, respectively.

According to the electromagnetic field theory, the electric field $\overline{E}$ can be computed as a function of the electric potential V and the magnetic vector potential $\overline{A}$ [2]:

$$\overline{E} = -\frac{\partial \overline{A}}{\partial t} - \text{grad}V. \tag{2}$$

The first term of equation (2), called "primary electric field – $\overline{E_A}$", is determined by means of the magnetic vector potential. For coils of non-traditional shapes, one can compute $\overline{A}$ using an approximation method in which the contour of the coil is first divided into a variable number of equal segments, and the magnetic vector potential in the calculus point is obtained by adding the contribution of each segment to the final value [2, 5].

The second term of (2) represents "the secondary electric field – $\overline{E_V}$". It depends on the geometry of the tissue-air boundary. A common application of magnetic stimulation is to excite peripheral nerves. The tissue-air interface is considered a flat surface. This term is computed knowing that on the surface, the boundary condition to be fulfilled is: $\overline{n} \cdot \overline{E}_A = -\overline{n} \cdot \overline{E}_V$ (continuity of the normal component of the current density vector, valid considering the fact that the regime of the electromagnetic field is quasistatic (f < 1 kHz) and therefore the time variation of the charge accumulated on the tissue-air boundary is zero). The electric field created by a flat surface charged with a certain charge density is $\overline{E} = \rho_S / 2\varepsilon_r \varepsilon_0$, and the charge accumulation occurs until the normal component of the primary electric field equals the normal component of the secondary electric field; therefore one can compute ρ_S as $\rho_S = -2 \cdot \varepsilon_r \cdot \varepsilon_0 \cdot \overline{n} \cdot \overline{E}_A$.

One of the major problems that appear in the design phase is the computation of the inductance of the stimulating coil. For simple shapes of the coils (circular), one can determine analytical computation formulas. When, however, the shape and

the spatial distribution of the coil's turns do not belong to one of the known structures, a numerical method needs to be used for determining the inductance.

The inductance is evaluated by taking the line integral of the vector potential around the coil, for unit current [5]: $L = \oint \overline{A} \cdot \mathrm{d}\overline{l}$. This formula permits the computation of inductances of the special coils, designed to improve focality.

The idea is to divide the coils in small segments (in our paper, each turn is divided in 64 equal segments). Starting from this method, two computation systems were developed by the authors of this paper:

- The first one is classical and it just consists of a software implementation (Matlab);
- The second one consists of realizing a hardware architecture that exploits the intrinsic parallelism of the problem. The physical support of this architecture is a FPGA device. Details about this implementation are given in section 3 of this paper.

The self-inductance of the circuit, divided in n parts, can be computed with formula (3). This mainly adds up the self-inductivities of the separate segments with the mutual inductivities of all the involved segments [3]:

$$L = \sum_{k=1}^{n} L_k + \sum_{k=1}^{n} \sum_{i=1}^{n} M_{ki}, \quad \text{for} \quad i \neq k. \tag{3}$$

The self inductance of a short straight conductor, with round cross-section, for low frequencies, is [3]:

$$L = \frac{\mu_0 l}{2\pi}\left(\ln\frac{2l}{r} - \frac{3}{4} + \frac{128}{45\pi}\frac{r}{l} - \frac{r^2}{4l^2} \right), \tag{4}$$

with l the length of the conductor, and r the radius of its cross-section.

The mutual inductance between two straight conductors converging into a point is evaluated as [3]:

$$M = \frac{\mu_0}{4\pi}\cos\varphi\left[a \ln\frac{a+b+c}{c+a-b} + b \ln\frac{a+b+c}{c+b-a} \right]. \tag{5}$$

The given quantities are represented in Fig. 1, with a and b representing the length of the conductors and φ the angle between them.

For the general case, we consider two conductor segments in space. The first segment is between points of coordinates (x_a, y_a, z_a) and (x_b, y_b, z_b), while the second segment is between points (x_c, y_c, z_c) and (x_d, y_d, z_d), see Fig. 2.

On the second segment, we consider a point of coordinates (x, y, z). The parametric equation of the second segment is:

$$\begin{cases} x(s) = x_c + (x_d - x_c)s, \\ y(s) = y_c + (y_d - y_c)s, \\ z(s) = z_c + (z_d - z_c)s. \end{cases} \tag{6}$$

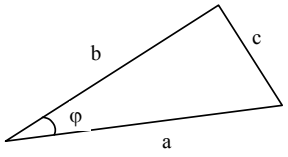

Fig. 1 – Computing the mutual inductance between two converging conductors.

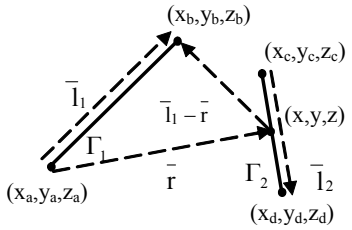

Fig. 2 – Two segments in space.

With the above geometrical coordinates, we can find the mutual inductance between these segments (using Neumann formula). For two circuits, Γ_1 and Γ_2, in an homogenous medium with permeability μ, the mutual magnetic flux Φ_{21} is:

$$\Phi_{21} = \int_{S_{\Gamma_2}} \overline{B}_{21} \mathrm{d}\overline{S} = \int_{\Gamma_2} \overline{A}_{21} \mathrm{d}\overline{l}_2. \tag{7}$$

Since circuits Γ_1 and Γ_2 are shaped like two straight segments, the mutual flux can be evaluated by integrating the magnetic vector potential created by the first segment along the second one. Considering the magnetic vector potential generated by a conductor segment, the mutual inductance can be computed using the following equation:

$$L_{21} = \frac{\mu_0}{4\pi} \cdot \oint_{\Gamma_2} \ln \frac{\left|\bar{l}_1 - \bar{r}\right| + l_1 - \dfrac{\bar{l}_1 \cdot \bar{r}}{l_1}}{r - \dfrac{\bar{l}_1 \cdot \bar{r}}{l_1}} \cdot \frac{\overline{l_1}}{l_1} \cdot \overline{\mathrm{d}l}_2. \tag{8}$$

The limits of the integral in equation (8) are given by: $s \in [0, 1]$.

To evaluate the correctness of our method, we compared the results obtained for the inductance of a multi-level circular coil with those computed analytically, with a formula provided in [1]. The results are in very good agreement (errors below 3% – the main source of errors is due to the fact that the numerical approach approximates each circular turn of the coil with a 64 sides regular polygon).

In order to asses the efficiency of energy transfer from the stimulator to the target biological tissue, we focus on stimulators with a fixed rise time of the current

$I(t)$ from 0 to peak, which is sufficient for comparing relative figures of merit of the stimulators.

The value of the coil's inductance, L, can be evaluated with the algorithm described above. The coil's resistance is:

$$R = 2\pi\eta A^{-1}\sum_{i=1}^{N} r_i, \tag{9}$$

where A is the cross-sectional area, η the resistivity of the wire and r_i the radius of the i-th loop.

Given the values of L and R, the capacitance C is obtained requiring that the rise time of the current is fixed ($\tau = 70$ μs).

Because of the same requirement, we may substitute $\mathrm{d}I/\mathrm{d}t$ with $\left(\mathrm{d}I/\mathrm{d}t\right)_{t=0} = U_0 / L$. Assuming that the activation of the nerve fibre occurs for a preset value of the electric field E, we obtain U_0, the necessary initial voltage on the capacitor that would lead to activation.

The energy dissipated in the circuit during one pulse of duration Δt is [1]:

$$W_J = R\int_0^{\Delta t} I^2(t)\mathrm{d}t. \tag{10}$$

The peak magnetic energy in the coil required to induce a given electric field is [1]:

$$W_B = \frac{1}{2} L I_{peak}^2 . \tag{11}$$

The temperature rise in the coil after one pulse of duration Δt is (assuming there is no cooling):

$$\Delta T = \frac{\eta}{c\sigma A^2}\int_0^{\Delta t} I^2(t)\,\mathrm{d}t, \tag{12}$$

where η is the resistivity, σ the density, c the specific heat and A the cross-sectional area of the copper wire of the coil.

These three quantities are evaluated to establish the parameters of energy transfer from the coil to the target tissue. The pulse duration Δt represents the period of the under-damped discharge current $I(t)$. Since the rise time of the current from zero to the peak value is τ, and it equals a quarter of a period, $\Delta t = 4 \cdot \tau = 280\,\mu\mathrm{s}$.

3. HARDWARE IMPLEMENTATION

The problem with the software implementation for computing the inductance of a coil is its running time. Coils are designed by trial-and-error, and this approach is impractical if each trial requires half a day of computation. Besides, as this time grows with the complexity of the coil, it prevents designing complex coils. The FPGA-based hardware acceleration is able to solve this bottleneck [4].

A Field-Programmable Gate Array (FPGA) is a semiconductor device containing programmable logic components ("logic blocks"), and programmable interconnectors. After the FPGA is manufactured, logic blocks can be programmed to perform simple or more complex functions. A hierarchy of programmable interconnectors allows logic blocks to be interconnected as needed by the system designer, somewhat like a one-chip programmable breadboard [4].

Several libraries of floating-point operators for FPGAs have been published in the last few years. In this work, we used FPLibrary, developed at Ecole Normale Supérieure de Lyon.

In Fig. 3, below, a block diagram of the system is displayed. Three main blocks can be distinguished. The most important block is the pipeline stage, which receives values, computes them, and in a final stage accumulates them.

The coordinates are stored in a Block RAM memory. The synchronization logic, which gives the data to the pipeline, is implemented in a special interface.

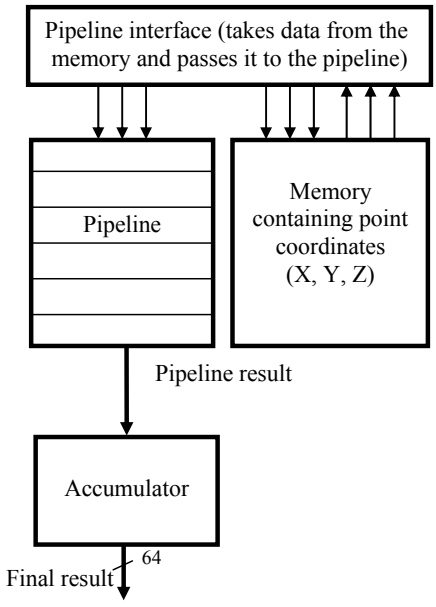

Fig. 3 – Architecture of the hardware system.

Our implementation has the advantage of greatly speeding up the computation time and hence shortening the design process. The performance and feasibility of the hardware implementation largely depends on its physical support. Our hardware platform was a Digilent Inc. board populated with a Xilinx Virtex2PRO30 FPGA device. The design occupies almost all the available space in the FPGA device and runs at 137 MHz (the maximum frequency reported for this implementation). This allowed us to achieve a performance that is at least two orders of magnitude superior to the software one.

4. RESULTS AND DISCUSSIONS

Considering a coil with N turns, the "Slinky-k" coils are generated by spatially locating these turns at successive angles of $i\sqrt{\times}180/(k-1)$ degrees, were $i = 0, 1,\ldots, k-1$ [3]. If the current passing through this coil is I, then the central leg carries the total current $N \times I$. With this definition, the circular coil is considered a "Slinky-1" coil, and two coplanar coils arranged in the shape of figure eight is a "Slinky-2" coil.

First, we considered a set of 5 coils with the same number of turns (8) and the same radius of the loop ($a = 38.1$ mm). The number of turns per loop is 8, for "Slinky-1", 4-4 for "Slinky-2", 2-4-2 for "Slinky-3"; 2-2-2-2 for "Slinky-4" and 1-2-2-2-1 for "Slinky-5". For each one, we used eq (2) to compute the total electric field along the $y = 0$ line (the Ox axis). The results obtained are given in Fig. 4.

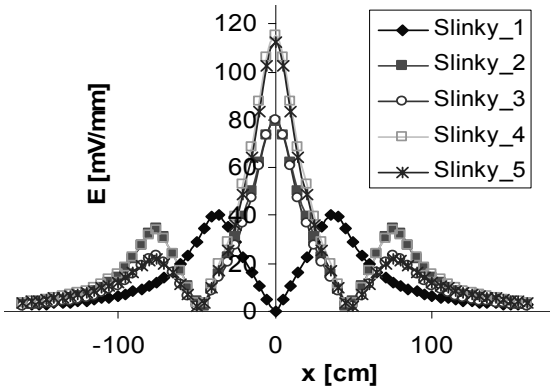

Fig. 4 – Electric field strength distribution, for the set of slinky 1 to 5 coils.

The focality criterion is given by the ratio between the primary and secondary peak of the total electric field. Therefore, focalization requires the maximization of

E in the center of the coil and minimization of the same quantity along the periphery. Table 1 gives the value of this ratio for the considered coils.

Table 1

Values of primary peak, secondary, and ratio

Coil	Primary peak mV/mm	Secondary peak mV/mm	Ratio
"Slinky-1"	40.1365	40.1365	1
"Slinky-2"	79.197	34.6578	2.28
"Slinky-3"	80.0244	23.2743	3.43
"Slinky-4"	115.1529	33.708	3.41
"Slinky-5"	112.3219	22.0538	5.09

Since from the set of coils initially considered, the "Slinky-5" has the best focality ratio, for this coil we tried to establish how the dimensions and position of the turns (the coil profile) influence its energetic parameters.

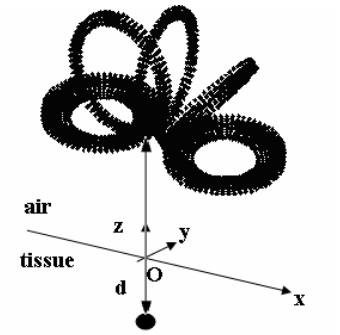

Fig. 6 – Slinky – 5 coil and the target point. The distance from the coil to the tissue-air interface is 5 mm in all cases.

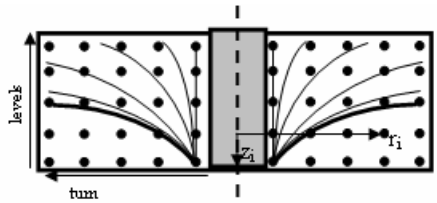

Fig. 7 – Distribution of turns on levels inside a circular coil.

From our previous work [5], one can conclude that the largest loop nearest the target induces the larger electric field. Therefore, for simple circular coils, the number of turns should decrease with the distance from the target (see auxiliary lines in Fig. 7). Analyzing the variation of energy consumed as a function of the turn radius, we established that the optimal value of this radius – the one that leads to the lowest energy consumption – is about 30 mm. For this value, the magnetic energy is minimal, and although the Joulean energy still decreases as the radius increases, this decrease is no longer significant.

Then, we considered 15 different configurations of a larger Slinky-5 coil. All these configurations respect the structure of the previous Slinky-5 coil (established to produce a more focal induced electric field [5]), having more turns on the horizontal leafs (leafs 1 and 5) than on the bended ones (leafs 2, 3 and 4). In the first 10 cases, there are 15 turns on each of the two horizontal directions and 7, respectively 6 turns on each of the three bended ones; the last 5 configurations have 16 turns on the two horizontal directions and 6 turns on each of the other leafs (a total number of 50 turns). These larger coils are necessary since most stimulators require that the coil's inductance is above 50 μH. Such a coil will have several turns, and therefore computing the inductance is a very long process using the software implementation of our algorithm. But the hardware one is able to solve this problem.

The geometrical parameters of the coil are: outer radius – 30mm, wire radius – 1mm and insulation gap between turns – 0.2 mm. Considering now that the activation threshold is set to 60 V/m in the target point – positioned 10 mm under the centre of the coil, table 2 presents the energetic parameters evaluated for these coils. The configuration section of table 2 gives only the number of turns and levels for the first, second and third leafs of the Sliky-5 coil. Leaf 4 is symmetrical with leaf 3 and leaf 5 is symmetrical with leaf 1. For example, the optimal coil, highlighted, has, on the first leaf: 6 turns on the first level, 5 turns on the second one and 4 turns on the third level; on the second leaf, we have: 3 turns on the first level, 3 on the second level and 1 on the third one, while the third leaf has 3 turns positioned on each of it's two levels.

Table 2

Energetic parameters of a set of Slinky–5 coils, on 15 geometrical configurations

Configuration	L [μH]	C [μF]	I_{peak} [A]	W_J [J]	W_B [J]	ΔT [°C]
15 – 7 – 6 –7 – 15	25.1	83.9330	582.1125	2.2752	4.2526	0.0227
5,5,5 – 4,3 – 3,3	54.8	37.4829	445.6087	1.7164	5.4407	0.0135
7,5,3 – 3,3,1 – 3,3	53.1	38.7129	447.0007	1.7102	5.3049	0.0136
7,5,3 – 4,3 -3,3	52.1	39.4825	452.0322	1.7476	5.3229	0.0139
7,4,4 – 4,3 – 3,3	53.6	38.3423	450.8147	1.7439	5.4467	0.0138
7,4,4 – 3,3,1 – 3,3	53.6	38.3515	445.6365	1.7151	5.3223	0.0135
6,6,3 – 4,3 –3,3	52.6	39.0971	450.1499	1.7375	5.3293	0.0138
6,6,3 – 3,3,1 – 3,3	53.8	38.2039	445.1026	1.7113	5.3293	0.0135
6,5,4 – 4,3 –3,3	53.8	38.2009	445.9108	1.7138	5.3487	0.0135
6,5,4 – 3,3,1 – 3,3	55.1	37.2776	440.9661	1.6884	5.3571	0.0132
16 – 6 – 6 – 6 – 16	23.7	89.0633	592.5514	2.2953	4.1607	0.0235
8,6,2 – 3,3 – 3,3	49.2	41.8725	460.9164	1.7853	5.2261	0.0144
8,5,3 – 3,3 – 3,3	50.7	40.5991	453.5377	1.7421	5.2144	0.0140
7,5,4 – 3,3 – 3,3	53.2	38.637	444.8308	1.6937	5.2635	0.0135
7,6,3 – 3,3 – 3,3	52	39.5546	449.0480	1.717	5.2427	0.0137

One can see that the space distribution of the turns can play a very important role on improving the energy transfer from the coil to the tissue. One can observe

that the energy dissipated in the circuit is 5.4 % lower for the most efficient configuration than for the least efficient one, and the coil heating per pulse is also 8.3 % smaller.

These results emphasize only the improvements brought to already optimized structures, because compared to a 50 turns Slinky-5 coil, positioned on the configuration 16-6-6-6-16 (all turns in one level), the improvement is even more significant (energy dissipated in the circuit is 36 % higher and coil heating per pulse is 78 % higher for this coil!).

It is also important to notice that for the given parameters, these optimised coils respect the technical constrains of the stimulator's circuit: $I_{peak} \leq 20$ kA, $\Delta T \leq 0.1\ ^{o}$C per pulse, required for repetitive stimulation [1].

5. CONCLUSIONS

This paper analysis the energetic efficiency of Slinky-5 coils used in magnetic stimulation. From the point of view of energy transfer from the coil to the target tissue, the circular coil and even the coil shaped in the form of figure of 8 coil, also called Slinky-2 coil, are much more efficient than the other Slinky coils. But since focality is also an important criterion to be considered when choosing a magnetic coil for a specific application, this paper analyses the optimal inner structure of a Slinky-5 coil, proved to be the one that produces an optimal focality of the induced electric field inside the tissue.

We establish that the maximum radius of the coil's leafs should be about 30mm, and analyze the role played by the space distribution of the turns on improving the energy transfer from the coil to the tissue. The conclusion is that optimization leads to a reduction of over 26 % in power consumption and of 43 % in coil heating per pulse, which can be an important step forward in designing coils for repetitive magnetic stimulation.

Therefore, one can conclude that the application is the one that sets the best design for the magnetic coil; there is no universal solution, suitable for all cases.

Received on 14 July, 2008

REFERENCES

1. J. Ruohonen, J. Virtanen, *Coil Optimisation for Magnetic Brain Stimulation*, Annals of Biomedical Engineering, **25** (1997).
2. B.J. Roth, P.J. Basser, *A Model of the Stimulation of a Nerve Fiber by Electromagnetic Induction*, IEEE Transactions on Biomedical Engineering, **37** (1990).
3. P.L Kalantarov, L.A. Țeitlin, *Calculul inductivităților*, Edit. Tehnică, Bucuresti, 1958.
4. D. Guell, T. El-Ghazawi, K. Gaj, V. Kindratenko. *High-Performance Reconfigurable Computing*, IEEE Computer, **40**, *3*, pp. 23-27 (2007).
5. L. Darabant, M. Pleşa, D. D. Micu, D. Ştef, R. Ciupa, A. Darabant, *Energy Efficient Coils for Magnetic Stimulation of Peripheral Nerve*, IEEE Transactions on Magnetics, **45**, *3*, pp. 1690-1693 (2009).